

# $\mu$ EDM machining of ZrB<sub>2</sub>-based ceramics reinforced with SiC fibres or whiskers

WCMNM  
2020

Quarto Mariangela<sup>1</sup> Bissacco Giuliano<sup>2</sup> D'Urso Gianluca<sup>1</sup>

<sup>1</sup> Dept. of Management, Information and Production Engineering, University of Bergamo, Via Pasubio 7/b, 24044 Dalmine (BG), Italy

<sup>2</sup> Dept. of Mechanical Engineering, Technical University of Denmark, Produktionstorvet, Building 427, 2800 Kgs. Lyngby, Denmark

## Abstract

The effects of different reinforcement shapes on stability and repeatability of micro-electrical discharge machining were experimentally investigated for Ultra-High Temperature Ceramics based on zirconium diboride (ZrB<sub>2</sub>) doped by SiC. Two reinforcement shapes, namely SiC short fibres and SiC whiskers were selected following their potential effects on mechanical properties and oxidation performance. Specific sets of process parameters were defined minimizing the short circuits in order to identify the best combination for different pulse types. The obtained results were then correlated with the energy per single discharge and the number of occurred discharges for all the combinations of material and pulse type. The pulse characterization was performed by recording pulses data by means of an oscilloscope, while the surface characteristics were defined by a 3D reconstruction. The results indicated how reinforcement shapes affect the energy efficiency of the process and change the surface topography.

**Keywords:** micro-EDM; UHTCs; machinability.

## 1. Introduction

Among the advanced ceramic materials, Ultra-High-Temperature ceramics (UHTCs) are characterized by excellent performance in extreme environments. This family of materials is based on borides (ZrB<sub>2</sub>, HfB<sub>2</sub>), carbide (ZrC, HfC, TaC) and nitrides (HfN), which are characterized by high melting point, high hardness and good oxidation resistance. ZrB<sub>2</sub>-based materials are of particular interest because of their suitable properties combination and are considered promising for several applications; for example, among the most attractive applications, one is in the aerospace sector as a component for the re-entry vehicles and devices [1,2]. In recent years, researchers are focused on fabricating high-density composites characterized by good strength (500-1000 MPa). In this respect, the relative density of the base material ZrB<sub>2</sub> is usually about 85% due to the high level of porosity of the structure. For these reasons, many efforts have been done on ZrB<sub>2</sub>-based composites in order to improve the mechanical properties, oxidation performances, and fracture toughness; however, the low fracture toughness remains one of the greatest efforts for the application of these materials under severe conditions [3,4]. Usually, the fracture toughness of ceramic materials can be improved by incorporating appropriate reinforcements that activate toughening mechanisms such as phase transformation, crack pinning, and deflection. An example is the addition of SiC. In fact, it has been widely proved that its addition improves the fracture strength and the oxidation resistance of ZrB<sub>2</sub>-based materials due to the grain refinement and the formation of a silica-based protective layer [5,6]. Despite all the studies that aim at improving mechanical properties and resistance, this group of materials is very difficult to machine by means of traditional technologies, because of their high hardness and brittleness. Only two groups of processes are effective in processing them: on one side the abrasive processes such as grinding, ultrasonic machining, and waterjet

machining, on the other side the thermal processes such as laser and electrical discharges machining (EDM) [7–11]. In this work, ZrB<sub>2</sub> materials containing 20% vol. SiC whiskers or fibres produced by hot pressing were machined by the  $\mu$ EDM process. This process was selected since its ability of work without generating mechanical stress and vibration, allowing the machining of fragile materials reducing the risk of fracture and cracks generation. In particular, the effects of the non-reactive reinforcement shapes on the process performance were investigated, verifying if the process is stable and repeatable. The choice of 20% vol. is related to the evidence reported in previous work [12], in which it was shown that this fraction of reinforcement allowed generating the best combination of oxidation resistance and mechanical characteristics useful for obtaining better results in terms of process performance and dimensional accuracy for features machined by micro-EDM.

## 2. Materials and Methods

### 2.1 Materials

ZrB<sub>2</sub> reinforced with 20% SiC short fibres (ZrB<sub>2</sub>0f) and ZrB<sub>2</sub> reinforced with 20% SiC whiskers (ZrB<sub>2</sub>0w), provided by ISTECC-CNR of Faenza (Italy), were selected for evaluating the influence of reinforcement shape on the process performance of  $\mu$ EDM technology.

ZrB<sub>2</sub> Grade B (H.C. Starck, Goslar, Germany), SiC HI Nicalon-chopped short fibres, characterized by 15  $\mu$ m diameter and 300  $\mu$ m length or SiC whiskers characterized by average diameter 1  $\mu$ m and average length 30  $\mu$ m were used for the preparation of the ceramic composite [13]. The powder mixtures were ball milled for 24 hours in pure ethanol using silicon carbide media. Subsequently, the slurries were dried in a rotary evaporator. Hot-pressing cycles were conducted in low vacuum (100 Pa) using induction-heated graphite die with a uniaxial pressure of 30 MPa during the heating and increased up to 50 MPa at  $T_{MAX}$  = 1700°C for fibres, and  $T_{MAX}$  = 1650°C for

whiskers. The maximum sintering temperature was set based on the shrinkage curve. Free cooling followed. After the preparation, the raw materials were analysed by Scanning Electron Microscopy (SEM). ZrB20f (relative density 94%) shows a very clear separation between the base matrix and the non-reactive reinforcement. Fibres dispersion into the matrix is homogenous and the fibres are characterized by the same orientation, as no agglomeration was observed in the sintered body. For ZrB20w, a dense microstructure (relative density about 97%) was observed and the whiskers are generally well dispersed into the matrix. These considerations are supported by the SEM-EDS analysis.

## 2.2 Experimental set-up

The effects of selected reinforcement shapes were investigated by conducting  $\mu$ EDM milling experiments. A simple circular pocket having a diameter equal to 1 mm and a depth of about 200  $\mu$ m was selected as the test feature. Solid tungsten carbide electrode with a diameter equal to 300  $\mu$ m and hydrocarbon oil were used as tool and dielectric fluid respectively. The experiments were performed for three different pulse shapes carrying out preliminary tests to define the optimal process parameters. The experimental campaign was based on a general full factorial design, featured by two factors: the reinforcement shape, defined by two levels, and the pulse type, defined by three levels. Different levels of pulse types identify differences in the peak of current reached during the machining and different duration of the discharges; in particular, level A is referred to long pulses while level C identify the short pulses and the average energy per discharge. Three repetitions were performed for each run. Since the machine used for experiments presents an autoregulating system, the characterization of electrical discharges is very important, not only to assess the real value of process parameters but, most of all, to evaluate the stability and repeatability of the process. An acquisition system was developed and used to collect waveforms for characterizing the process. A current monitor with a bandwidth of 200 MHz and a voltage probe were connected to the  $\mu$ EDM machine and to a programmable counter and a digital oscilloscope. These connections allow the acquisition of the current waveforms and count the occurred discharges (1 minute of acquisition) with a real-time sample rate of 40 MSa/s. The trigger on the counter was set to a value of 0.5 A to avoid the influence of the background noise on discharge counting. Through the Matlab data elaboration, it was possible to calculate the numbers of electrical discharges, their instantaneous values, width, and voltage. Finally, the average value of energy per discharge (E) was estimated by integrating the instantaneous value of the power, calculated as the product of the instantaneous values of current ( $i(t)$ ) and voltage ( $v(t)$ ), with respect to the time. The discharge population distributions as a function of reinforcement shape and pulse type applied to the machining is well represented by a normal distribution which suggests a good reproducibility and stability of the process. The experimental set-up is reported in Fig. 1.

## 2.3 Characterization procedure

A 3D reconstruction of micro-slots was performed by

means of a confocal laser scanning microscope with a magnification of 20x. The obtained images were analysed with software SPIP by Image Metrology. A plane correction was performed on all the images to level the surfaces and to remove primary profiles; then, the arithmetic mean roughness ( $S_a$ ) was assessed by the real-topography method, based on the international standard UNI EN ISO 25178:2017. The process performances were evaluated through the estimation of Material Removal per Discharge ( $MRD$ ), estimated taking into account the relative density ( $\delta$ ) ( $MRD_\delta$ ) for adjusting the volume of the micro-slots ( $MRT$ ) for compensating the presence of porosity in the sample structure and Tool Wear per Discharge ( $TWD$ ), estimated as the ratio between the volume of electrode wear ( $MRT$ ) and the number of discharges recorded by the programmable counter. Then, the Tool Wear Ratio ( $TWR_\delta$ ) was calculated as the ratio between the previous performance indicators, considering the relative density of the workpiece material.

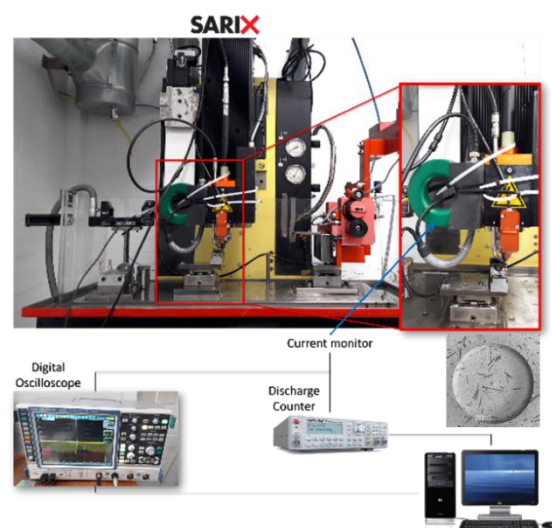


Fig. 1. Experimental set-up scheme.

## 3. Results and discussion

Considering both reinforcement shapes, the intensity of the pulses are included in a similar range for pulses type A and B, while, for a short pulse, they are characterized by some differences: for whiskers, the maximum peak current corresponds to the average value of the peaks occurred for the short fibres.

In terms of peaks of current and voltage, the only relevant difference can be remarked for energy per discharge, in fact, the discharges developed during the machining on the ZrB20w generate slightly higher energy in comparison to the energy per discharge of ZrB20f. In particular, the energy per discharge generated by pulse type A for ZrB20w is 0.72% higher than the energy developed by the same pulse type for ZrB20f. This is a very tiny difference, but considering the pulse type C, the energy per discharge developed is about 45% higher than the energy generated by the same pulse type for fibres.

The distribution of energy is discussed, analysing the efficiency in terms of specific removal energy. Fig. 2 (a) shows the ratio between  $TWD$  and the energy of single discharge ( $TWD_E$ ) as a function of the reinforcement fraction and the pulse type. In the same

way, the  $MRD_{\delta}$  was related to the energy of a single discharge to evaluate the energy efficiency from the material removed point of view ( $MRD_{\delta/E}$ ). In both cases (Fig. 2 (a) and (b)), pulse type A shows a lower efficiency; in other words, this means that most of the energy developed in a single discharge was lost. In this case, the pulse type C is characterized by a higher fraction of energy dedicated to the material removal from the workpiece, despite pulse type C is being characterized by very short duration and low energy (Fig. 2 (b)). Despite the great difference in energy per discharge, this shows that the pulse type C directs most of the energy towards the workpiece. Fig. 2 (c) shows that the  $TWR_{\delta}$  for all pulse types is lower for specimens containing whiskers. In particular, the whiskers show a better performance allowing to reduce the tool wear and to increase the material

removal rate efficiency. The intermediate position of pulse type C identified in Fig. 2 (a) can be related to a different energy distribution. In particular, which energy fraction is dedicated to the material removal from the workpiece. The factorial design was analysed in order to comprehend which factors and interactions are statistically significant for the performance indicators and surface roughness. A general linear model was used to perform a univariate analysis of variance, including all the main factors and their interactions. The ANOVA analysis is performed applying a confidence interval of 95%. As a general remark, all the indicators resulted to be influenced by both the reinforcement shape and the pulse type. For  $MRD_{\delta}$  and  $TWD$ , also the interaction showed an effect in terms of ANOVA (Table 1). This aspect suggested that the interaction of factors is relevant for indicators that can be correlated to the machining duration.

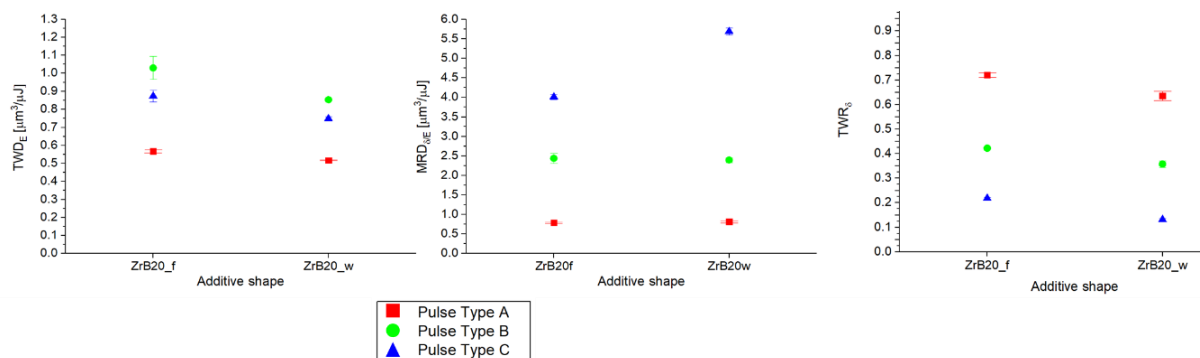


Fig. 2. Average values and standard deviation as a function of reinforcement shape and pulse type.

Main effects plots (Fig. 3) show that indicators are mainly influenced by the pulse type that establishes the range in which process parameters can vary, and in particular, the characteristics of the pulses. For all indicators, reduction in pulse duration and peak current intensity generate the lower value of  $MRD_{\delta}$ ,  $TWD$ , and  $TWR_{\delta}$ . At the same time, tests with whiskers reinforcement generate an improvement in  $MRD_{\delta}$  and in surface finishing while giving rise to a reduction in  $TWD$  and  $TWR_{\delta}$ . By increasing the pulse duration and the peak intensity from type C to type A, the  $MRD_{\delta}$  is 10 times greater, but the surface quality decreases by -60%. For  $MRD_{\delta}$  and  $TWD$ , also the interaction between pulse type and reinforcement shape affects the results. In particular, when the samples are machined by pulse type C, the effect on  $MRD_{\delta}$  is more evident, while from the  $TWD$  point of view it is more evident for pulse type A (Fig. 4). In general, tests performed on materials with whiskers reinforcement are characterized by better results, both in terms of process performances and surface finishing.

occurred on UHTCs, in particular when there is a low-electrically conductive part in the structure. Fig. 5(a) represents a portion of the machined area on ZrB20f where it is possible to identify a sort of “protrusion” in correspondence of the fibres. This is probably related to not complete machining because of the SiC low electrical conductivity characteristic and the great extension of the area of the fibre. Sample containing whiskers show a uniform and homogeneous surface due to the better dispersion of SiC particles (Fig. 5(b)).

Table 1. Analysis of Variance p-values.

	FACTORS		
	Pulse Type	Shape	Interaction
$MRD_{\delta}$	<b>0.000</b>	<b><math>1.21 \cdot 10^{-4}</math></b>	<b>0.030</b>
$TWD$	<b>0.000</b>	<b>0.000</b>	<b><math>4.51 \cdot 10^{-5}</math></b>
$TWR_{\delta}$	<b>0.000</b>	<b>0.000</b>	0.202
Sa	<b>0.000</b>	<b>0.005</b>	0.156



Fig. 3. Main effects plot for indicators affected by pulse type and reinforcement shape.

These aspects justify the different results obtained in terms of surface quality and, in general, these different textures can be considered a starting point for further studies about the material removal mechanism that

In addition to this, the SEM observations SEM (Fig. 6) show higher fragmentation of the recast layer for ZrB20w. This aspect is particularly evident on surfaces machined by long pulses; in fact, for pulse type A and B, the surface is for the major part covered by recast materials for both reinforcement shapes, but ZrB20w

presents smaller extensions of the single “crater” of recast materials. A different behaviour can be observed for surfaces machined by the short pulses. In this case, for ZrB<sub>2</sub>of can be observed a smaller area of recast material, probably due to the combination of the greater dimensions of the fibres (in comparison to the whiskers), the lower energy per discharge for short pulses and the low electrical conductivity of the SiC. In particular, the fibres have a bigger surface and it needs to remove the entire parts (cause of protrusion generation).

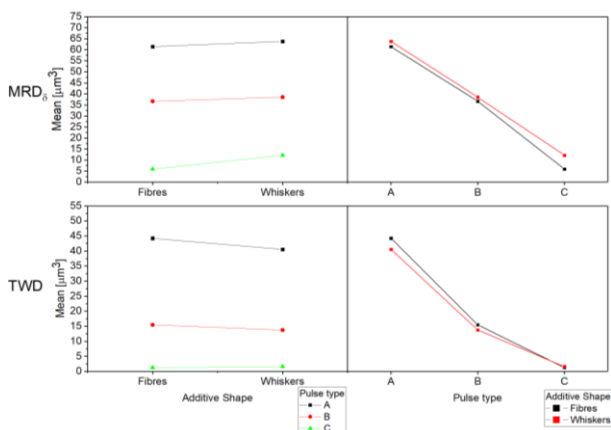


Fig. 4. Interaction plot for MRD $\delta$  and TWD.

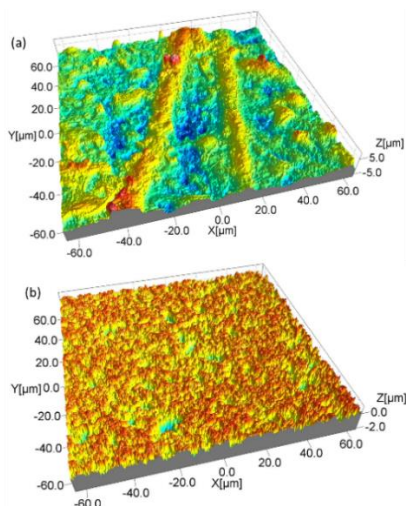


Fig. 5. Details of machined surfaces for ZrB<sub>2</sub>of (a) and ZrB<sub>2</sub>0w (b) machined by pulse type A.

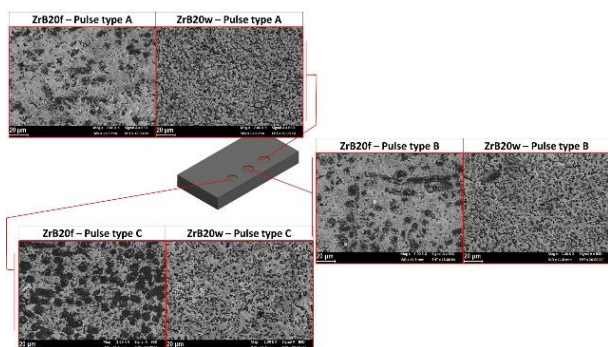


Fig. 6. SEM backscatter images of the machined surface.

#### 4. Conclusions

Machinability evaluation of ZrB<sub>2</sub>-based composites hot-pressed with two different shapes non-reactive

reinforcement (SiC) was performed in this work. Stability and repeatability of the  $\mu$ EDM were evaluated to identify the effects of the reinforcement shapes taking into account the process performances and surface finishing. First of all, a discharge characterization was performed to feature the different pulse type used during the machining. In general, the discharge characterization and the performances indicators identify a stable and repeatable process with a faster material removal for samples doped with whiskers. The analysis of variance showed that both factors are statistically significant for the indicators selected in the process evaluation and in general, the use of whiskers improves the machining efficiency generating lower tool wear. Furthermore, the interaction between the two factors turns out to be influential only for MRD and TWD, which are indirectly related to the machining duration, since the number of discharges occurred during the machining was considered in their estimation. This investigation shows that the specimens having a 20 vol.% of reinforcement in form of whiskers results to be the best solution in terms of machinability by EDM process not only for the better process performances (high MRD and low TWD), but also for the higher level of surface quality, an essential criterion for making a proper decision in an industrial environment.

#### Acknowledgements

The authors would like to thank D. Sciti and L. Silvestroni from ISTECC – CNR of Faenza (Italy) for the production and supply of the materials used in this study.

#### References

- [1] Saccone G, Gardi R, Alfano D, Ferrigno A, Del Vecchio A. Laboratory, on-ground and in-flight investigation of ultra high temperature ceramic composite materials. *Aerosp Technol* 2016;**58**:490–497.
- [2] Justin JF, Jankowiak A. Ultra High Temperature Ceramics: Densification, Properties and Thermal Stability. *AerospaceLab J* 2011;**3**(3):AL3-08.
- [3] Zhang P, Hu P, Zhang X, Han J, Meng S. Processing and characterization of ZrB<sub>2</sub>-SiCw ultra-high temperature ceramics. *J Alloys Compd* 2009;**472**(1–2):358–362.
- [4] Yang F, Zhang X, Han J, Du S. Characterization of hot-pressed short carbon fiber reinforced ZrB<sub>2</sub>-SiCw ultra-high temperature ceramic composites. *J Alloys Compd* 2009;**472**(1–2):395–399.
- [5] Zhang X, Xu L, Du S, Han J, Hu P, Han W. Fabrication and mechanical properties of ZrB<sub>2</sub>-SiCw ceramic matrix composite. *Mater Lett* 2008;**62**(6–7):1058–1060.
- [6] Tian WB, Kan YM, Zhang GJ, Wang PL. Effect of carbon nanotubes on the properties of ZrB<sub>2</sub>-SiC ceramics. *Mater Sci Eng A* 2008;**487**(1–2):568–573.
- [7] Hwang SS, Vasiliev AL, Padture NP. Improved processing and oxidation-resistance of ZrB<sub>2</sub> ultra-high temperature ceramics containing SiC nanodispersoids. *Mater Sci Eng A* 2007;**464**(1–2):216–224.
- [8] Samant AN, Dahotre NB. Laser machining of structural ceramics-A review. *J Eur Ceram Soc* 2009;**29**(6):969–993.
- [9] Samant A. Laser Machining of Structural Ceramics: Computational and Laser Machining of Structural Ceramics: Computational and Experimental Analysis Experimental Analysis. 2009. [https://trace.tennessee.edu/utk\\_graddiss](https://trace.tennessee.edu/utk_graddiss) (accessed 19 Jul 2021).
- [10] Rakshit R, Das AK. A review on cutting of industrial ceramic materials. *Precis Eng* 2019;**59**:90–109.
- [11] D’Urso G, Giardini C, Quarto M. Characterization of surfaces obtained by micro-EDM milling on steel and ceramic components. *Int J Adv Manuf Technol* 2018;**97**(5–8):2077–2085.
- [12] Quarto M, Bissacco G, D’Urso G, D’Urso G. Machinability and Energy Efficiency in Micro-EDM Milling of Zirconium Boride Reinforced with Silicon Carbide Fibers. *Materials (Basel)* 2019;**12**(23):3920.
- [13] Silvestroni L, Sciti D, Melandri C, Guicciardi S. Toughened ZrB<sub>2</sub>-based ceramics through SiC whisker or SiC chopped fiber additions. *J Eur Ceram Soc* 2010;**30**(11):2155–2164.